Technical Report 1323
November 1989

Application of Frequency Interpolation to Acoustic-Structure Interaction Problems

G. W. Benthien

NAVAL OCEAN SYSTEMS CENTER

San Diego, California 92152-5000

J. D. FONTANA, CAPT, USN
Commander

R. M. HILLYER
Technical Director

ADMINISTRATIVE INFORMATION

This work was performed by the Transduction Sciences Branch, Code 712, Naval Ocean Systems Center, for the Naval Research Laboratory as part of the Target Physics Block Program sponsored by the Office of Naval Technology.

Released by
C. L. Meland, Head
Transduction Sciences Branch

Under authority of
T. F. Ball, Head
Acoustic Systems and
Technology Division

ACKNOWLEDGMENTS

The author would like to thank Don Barach and David Gillette for converting the techniques described in this report into efficient computer programs and for obtaining the included numerical results. The author would also like to thank H. A. Schenck for his review of this paper and for many useful discussions and suggestions.

JG

SUMMARY

For coupled structural acoustic scattering problems, the spectral response often varies rapidly over a large dynamic range, requiring the response to be calculated at many closely spaced frequencies. In such problems, the computation time is often dominated by the calculation of acoustic interactions which do not vary rapidly with frequency. It is shown in this report that large savings in computation time can be achieved without significant loss of accuracy by interpolating on appropriately scaled intermediate acoustic quantities. These quantities are computed on a coarse frequency grid and then interpolated to any desired frequency resolution in order to obtain the final response. The overall savings in computation time is typically more than an order of magnitude.

CONTENTS

FIGURES

TABLE

INTRODUCTION

A technique for solving acoustic-structure interaction problems was described in a previous Naval Ocean Systems Center (NOSC) technical report (Schenck and Benthien, 1989). In this technique the elastic structure is modeled using the finite element method, and the acoustic field is modeled using the Combined Helmholtz Integral Equation Formulation (CHIEF) (Schenck, 1968). The purpose of this report is to describe a frequency interpolation scheme for improving the computational efficiency of this numerical technique.

Due to the resonant nature of the elastic structure, it is often necessary to compute the acoustic field at a large number of closely spaced frequencies. In such problems the computational time is dominated by the acoustic calculations. It will be shown that the computational time can be reduced considerably by interpolating on certain scaled acoustic quantities which vary slowly with frequency. Furthermore, it will be shown that this frequency interpolation scheme results in little, if any, loss of accuracy.

The second section of this report contains a brief summary of the basic equations involved in the numerical solution of acoustic-structure interaction problems. The third section contains a description of the frequency interpolation scheme as it is applied to certain appropriately scaled acoustic quantities. The fourth section contains results from two example problems which illustrate the accuracy and computational efficiency of the frequency interpolation scheme. Such improvements in computational efficiency should be very important as one attempts to employ this numerical technique at higher frequencies where computation times can be quite large. The last section summarizes the results of this work.

BASIC EQUATIONS

Throughout this section all pressures, displacements, and velocities will be represented by their complex, frequency dependent Fourier components corresponding to the time dependence $e^{i\omega t}$. The elastic structure is modeled using the finite element equations (Zienkiewicz, 1977)

$$(-\omega^2 M + K)U = F^{rad} + F^D, \tag{1}$$

where M is the mass matrix, K is the stiffness matrix, F^{rad} is the load vector corresponding to acoustic loading, F^D is the load vector corresponding to nonacoustic mechanical drive forces on the structure, and U is a column vector whose components are the displacement degrees-of-freedom at all the nodes in the body. The components of F^{rad} are given by

$$F_m^{rad} = -\int_S p\,\boldsymbol{\phi}_m \cdot \boldsymbol{n}\, dS, \tag{2}$$

where p is the acoustic pressure, $\boldsymbol{n}$ is a unit normal to the wet-surface S pointing into the fluid, and $\boldsymbol{\phi}_m$ is a finite-element vector interpolation function. The displacement $\boldsymbol{u}(x)$ at a point x in the body can be expressed in terms of the interpolation functions $\boldsymbol{\phi}_m$ as follows:

$$\boldsymbol{u}(x) \doteq \sum_{m=1}^{M} U_m \boldsymbol{\phi}_m(x), \tag{3}$$

where $U_1, \ldots, U_M$ are the components of U.

The CHIEF formulation for the acoustic field is based on the Helmholtz integral relations. The scalar acoustic wave equation for the acoustic medium is replaced by an integral equation over the wet-surface S which in turn is approximated by a system of algebraic equations (Benthien, Barach, and Gillette, 1988)

$$AP = BV + P^{inc}, \tag{4}$$

where P and V are column vectors whose nth components are the pressure and normal velocity (assumed to be constant) on the nth subdivision S_n of S; and P^{inc} is a column vector whose nth component is the value of the incident pressure wave at a reference point on S_n. (For acoustic radiation problems $P^{inc} = 0$.) The matrices A and B in equation (4) have components given by

$$A_{mn} = \tfrac{1}{2}\delta_{mn} - \int_{S_n} \frac{\partial G(\zeta_m, \sigma)}{\partial n_\sigma}\, dS(\sigma) \tag{5}$$

$$B_{mn} = i\omega\rho \int_{S_n} G(\zeta_m, \sigma)\, dS(\sigma), \tag{6}$$

where δ_{mn} is the Kronecker delta, ζ_m is a reference point on S_m, and $G(\zeta_m, \sigma)$ is the free-space Green's function

$$\begin{aligned} G(\zeta_m, \sigma) &= \frac{e^{-ikr(\zeta_m,\sigma)}}{4\pi r(\zeta_m, \sigma)} \qquad (k = \omega/c) \\ r(\zeta_m, \sigma) &= \text{the distance between } \zeta_m \text{ and } \sigma. \end{aligned} \tag{7}$$

The normal derivative of $G(\zeta_m, \sigma)$ is given by the expression

$$\frac{\partial G(\zeta_m, \sigma)}{\partial n_\sigma} = -\frac{G(\zeta_m, \sigma)}{r^2(\zeta_m, \sigma)} \left(ik + \frac{1}{r(\zeta_m, \sigma)} \right) [(\sigma - \zeta_m) \cdot \boldsymbol{n}(\sigma)]. \tag{8}$$

It is well known that the solution of the Helmholtz integral equation for p in terms of v and p^{inc} is not unique at certain frequencies corresponding to the eigenfrequencies of the interior Dirichlet problem. In the neighborhood of these eigenfrequencies the matrix A in equation (4) becomes ill-conditioned. To overcome this numerical difficulty, CHIEF (Schenck, 1968) supplements the equations in (4) by additional equations of the same form in which each ζ_m is a point interior to S. The resulting overdetermined system of equations has a unique solution in the least-squares sense.

The total acoustic pressure p in the field can be written as the sum of the incident pressure p^{inc} and the scattered pressure p^s, i.e.,

$$p(x) = p^{inc}(x) + p^s(x). \tag{9}$$

For radiation problems $p^{inc} = 0$ and $p = p^s$. The scattered pressure p^s at a field point x exterior to the structure can be approximated by

$$p^s(x) = a^T(x)P + b^T(x)V, \tag{10}$$

where $a(x)$ and $b(x)$ are column vectors having components given by

$$a_n(x) = \int_{S_n} \frac{\partial G(x, \sigma)}{\partial n_\sigma} \, dS(\sigma) \tag{11}$$

$$b_n(x) = i\omega\rho \int_{S_n} G(x, \sigma) \, dS(\sigma). \tag{12}$$

In the farfield of S, the components $a_n(x)$ and $b_n(x)$ can be approximated by

$$a_n(x) \doteq \frac{ike^{-ikR}}{4\pi R} \int_{S_n} (\hat{\boldsymbol{r}}(x) \cdot \boldsymbol{n}(\sigma)) e^{ik\hat{\boldsymbol{r}}(x)\cdot\boldsymbol{\delta}(\sigma)} \, dS(\sigma) \tag{13}$$

$$b_n(x) \doteq \frac{i\omega\rho e^{-ikR}}{4\pi R} \int_{S_n} e^{ik\hat{\boldsymbol{r}}(x)\cdot\boldsymbol{\delta}(\sigma)} \, dS(\sigma), \tag{14}$$

where R is the distance from an origin near the surface S to the field point x, $\hat{\boldsymbol{r}}(x)$ is a unit vector at the origin in the direction of x, and $\boldsymbol{\delta}(\sigma)$ is the position vector of the integration point σ relative to the origin .

Equations (4) and (10) can be combined to give

$$p^s(x) = q^T(x)V + p^{rs}(x), \tag{15}$$

where

$$q^T(x) = a^T(x)A^{-1}B + b^T(x)$$

and

$$p^{rs}(x) = a^T(x)A^{-1}P^{\text{inc}}.$$

It can be seen from equation (15) that $p^{rs}(x)$ is the rigid scattering from the body (i.e., the scattered pressure when V is constrained to be zero).

Applying the assumption that p is piecewise constant on the subdivisions of S to equation (2), gives

$$F^{rad} = -CDP, \tag{16}$$

where

$$C_{mn} = \frac{1}{S_n}\int_{S_n} \boldsymbol{\phi}_m \cdot \boldsymbol{n}\, dS$$

and

$$D = \text{diag}(S_1, S_2, \ldots, S_N).$$

Equations (1) and (16) can be combined to give

$$U = -(-\omega^2 M + K)^{-1}CDP + (-\omega^2 M + K)^{-1}F^D. \tag{17}$$

Since different interpolation schemes are used in the finite element model of the structure and the CHIEF model of the acoustic field, it is impossible to enforce exact continuity of normal displacement across S. However, this continuity is approximately enforced by equating the CHIEF normal velocity v_n to the average of the finite element normal velocity over S_n, i.e.,

$$v_n = \frac{1}{S_n}\int_{S_n} i\omega \boldsymbol{u} \cdot \boldsymbol{n}\, dS. \tag{18}$$

Combination of equations (3),(17), and (18) gives

$$\begin{aligned} V &= i\omega C^T U \\ &= -i\omega C^T(-\omega^2 M + K)^{-1}CDP + i\omega C^T(-\omega^2 M + K)^{-1}F^D. \end{aligned} \tag{19}$$

Let E be a matrix whose columns are the *in vacuo* normal modes of the structure, i.e.,

$$KE = ME\Omega, \tag{20}$$

where $\Omega = \text{diag}(\omega_1^2, \ldots, \omega_M^2)$ is the diagonal matrix of eigenfrequencies. Since the modes are M-orthogonal, they can be normalized so that

$$E^T M E = I. \tag{21}$$

It is easily verified that the inverse matrix $(-\omega^2 M + K)^{-1}$ can be expressed in terms of the normal mode matrix E as follows:

$$(-\omega^2 M + K)^{-1} = E(-\omega^2 I + \Omega)^{-1} E^T. \tag{22}$$

This form is convenient since the diagonal matrix $(-\omega^2 I + \Omega)$ is easily inverted at all frequencies.

Combination of equations (19) and (22) gives

$$V = -i\omega C^T E(-\omega^2 I + \Omega)^{-1} E^T C D P + i\omega C^T E(-\omega^2 I + \Omega)^{-1} E^T F^D. \tag{23}$$

Equations (4) and (23) can now be combined to give

$$HP = P^{inc} + i\omega B C^T E(-\omega^2 I + \Omega)^{-1} E^T F^D, \tag{24}$$

where

$$H = A + i\omega B C^T E(-\omega^2 I + \Omega)^{-1} E^T C D.$$

Equation (24) can be solved for the surface pressure vector P. Once P is determined, the velocity vector V can be obtained from equation (23) and the scattered pressure $p^s(x)$ can be computed at any exterior field point x using equation (10) or equation (15).

FREQUENCY INTERPOLATION

In this section certain scaled acoustic quantities will be constructed which vary slowly with frequency. These scaled quantities can be computed with a coarser frequency resolution than is desired in the final frequency sweep, and the intermediate frequency values can then be obtained by interpolation. The only acoustic quantities involved in the system of equations (24) for P are the matrices A and B. It can be seen from equations (5) to (8) that the components of A and B both involve the quantity e^{-ikr} which varies rapidly with frequency when the separation is large. This rapid variation in the integrands of A_{mn} and B_{mn} can be eliminated by factoring out the quantity $e^{-ikr_{mn}}$ where r_{mn} is the distance between the reference points on S_m and S_n. Thus, the matrices $\hat{A}$ and $\hat{B}$ defined by

$$\hat{A}_{mn} = e^{ikr_{mn}} \int_{S_n} \frac{\partial G(\zeta_m, \sigma)}{\partial n_\sigma} \, dS(\sigma) \tag{25}$$

$$\hat{B}_{mn} = i\omega\rho e^{ikr_{mn}} \int_{S_n} G(\zeta_m, \sigma) \, dS(\sigma) \tag{26}$$

are slowly varying with frequency and are simply related to A and B by

$$A_{mn} = \tfrac{1}{2}\delta_{mn} - e^{-ikr_{mn}} \hat{A}_{mn} \tag{27}$$

$$B_{mn} = e^{-ikr_{mn}} \hat{B}_{mn} \quad . \tag{28}$$

Linear frequency interpolation can be used on $\hat{A}$, $\hat{B}$ and the matrices A, B can be recovered using equations (27) and (28).

The far-field calculations involve the acoustic quantities $a_n(x)$, $b_n(x)$ defined by equations (13) and (14). If $\boldsymbol{\delta}(\sigma)$ in these equations is approximated by $\boldsymbol{\delta}_n = \zeta_n - 0$, then equations (13) and (14) reduce to

$$a_n(x) = \frac{ik}{4\pi} \frac{e^{-ikR}}{R} e^{ik\hat{\boldsymbol{r}}(x)\cdot\boldsymbol{\delta}_n} \int_{S_n} \hat{\boldsymbol{r}}(x) \cdot \boldsymbol{n}(\sigma) \, dS(\sigma) \tag{29}$$

$$b_n(x) = \frac{i\omega\rho}{4\pi} \frac{e^{-ikR}}{R} e^{ik\hat{\boldsymbol{r}}(x)\cdot\boldsymbol{\delta}_n} S_n. \tag{30}$$

For equal frequency increments the quantity $e^{-ikr_{mn}}$ occurring in equations (27) and (28) and the quantity $e^{ik\hat{\boldsymbol{r}}(x)\cdot\boldsymbol{\delta}_n}$ occurring in equations (29) and (30) can be computed recursively using

$$e^{i(k+\Delta k)r} = e^{ikr} \cdot e^{i\Delta kr}. \tag{31}$$

The interpolation scheme can now be summarized as follows:

1. The matrices $\hat{A}$ and $\hat{B}$ defined in equations (25) and (26) are computed at a set of frequencies which have a wider spacing than the intended final frequency sweep.

2. The integrals $\int_{S_n} \hat{\boldsymbol{r}}(x) \cdot \boldsymbol{n}(\sigma)\, dS(\sigma)$ occurring in equation (29) are computed for each subdivision S_n and each desired far-field point x.

3. The exponentials $e^{-ikr_{mn}}$ and $e^{ik\hat{\boldsymbol{r}}(x)\cdot\boldsymbol{\delta}_n}$ are computed for a starting wavenumber k_0 and a wavenumber increment Δk corresponding to the final frequency resolution desired.

4. At each wavenumber $k_n = k_0 + (n-1)\Delta k$ the matrices $\hat{A}$ and $\hat{B}$ are computed using linear frequency interpolation.

5. The quantities $e^{-ikr_{mn}}$ and $e^{ik\hat{\boldsymbol{r}}(x)\cdot\boldsymbol{\delta}_n}$ are updated using the recursion relation (31).

6. The matrices A and B corresponding to k_n are computed using equations (27) and (28).

7. Equation (24) is solved for the surface pressures P.

8. The surface normal velocities V are computed using equation (23).

9. The far-field quantities $a_n(x)$ and $b_n(x)$ are computed using the equations (29) and (30).

10. The far-field pressure $p^s(x)$ is computed for each field point x using equation (10).

Examples will be shown in the next section which illustrate the accuracy and improvement in computational efficiency that can be obtained using this scheme.

NUMERICAL RESULTS

In this section two examples will be presented which illustrate the accuracy and improvement in computational efficiency that can be obtained using frequency interpolation. The first example involves the backscattering from a spherical shell. The ratio of the thickness to the mean radius of the shell is 0.03 . The material parameters of the shell are

- Density = 7669 Kg/m^3
- Young's modulus = 2.07×10^{11} N/m^2
- Poisson's ratio = 0.3 .

The material parameters of the water are

- Density = 998 Kg/m^3
- Sound Speed = 1486 m/s.

Figure 1 shows the backscattered form function for this spherical shell versus the normalized frequency ka for increasingly coarse interpolation in ka. The normalized frequency ka is defined by $ka = 2\pi fa/c$ where f is the frequency, a is the mean radius, and c is the sound speed in water. The ka increment Δka used in the acoustic calculations (CHIEF) was taken successively to be 0.01, 0.1, 0.2, 0.3. It can be seen from figure 1 that there was only a modest decrease in accuracy as Δka was increased. Table 1 shows the number of frequencies at which the CHIEF calculations needed to be made for each value of Δka.

Table 1. Number of CHIEF frequencies
required for sphere backscattering problem.

Δka	CHIEF Frequencies
0.01	141
0.10	15
0.20	8
0.30	6

As would be expected, the decrease in the number of CHIEF calculations results in a large reduction in overall computation time. Figure 2 shows the central processing unit (CPU) times required on a CONVEX CS-1 minisupercomputer for 100 frequencies and 91 far-field angles as a function of maximum ka. The top curve shows the CPU time required for the acoustic calculations with no frequency interpolation ($\Delta ka = .01$). The next lower curve gives the total (acoustic, finite-element, and coupling) CPU time required when $\Delta ka = 0.2$. The remaining curves show the CPU times for various parts of the calculation. With the new interpolation scheme, the time is dominated at low ka by the portion of the program which couples the CHIEF and finite element results. At higher ka the finite element computations dominate. In general, the frequency interpolation scheme has resulted in an overall reduction in computation time of about 15:1.

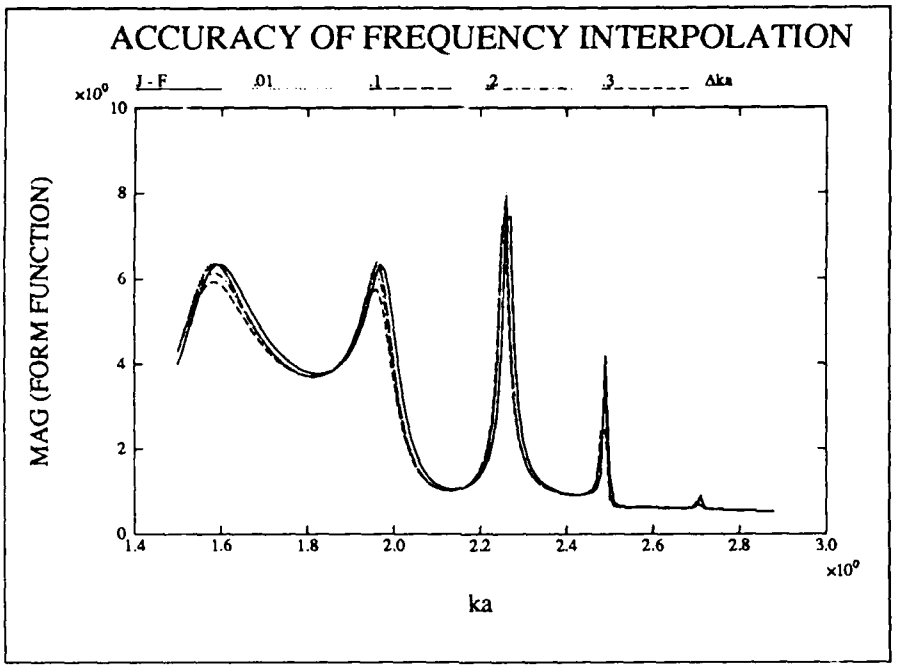

Figure 1. Backscattering from spherical shell utilizing frequency interpolation.

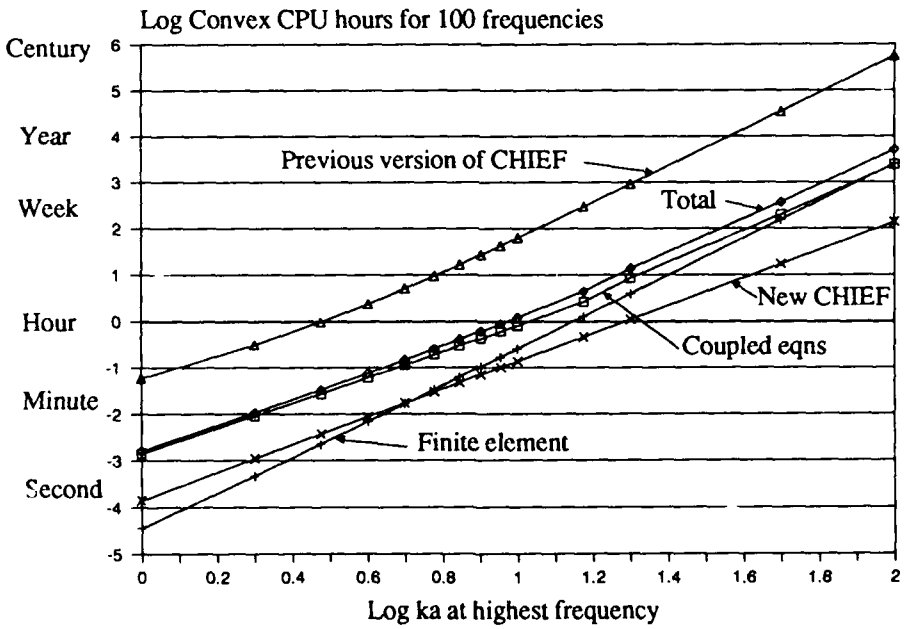

Figure 2. CPU time versus ka – with and without frequency interpolation.

The second example involves the backscattering off the end of a capped cylindrical shell. The ratio of the mean radius a to the length L of the shell is 0.125, and the ratio of the thickness h to the mean radius a of the shell is 0.01016 . The ends of the cylinder are capped with circular disks having the same thickness as the shell. The material properties of both the shell and endcaps are

- Density = 8977 Kg/m^3
- Young's modulus = 2.09×10^{11} N/m^2
- Poisson's ratio = 0.308.

The material parameters of the water are

- Density = 998 Kg/m^3
- Sound Speed = 1486 m/s.

Figure 3 shows the backscattered normalized pressure for an incident plane wave travelling along the axis of the cylinder. The scattered pressure is normalized by the high-frequency plane-wave approximation to the rigid backscattered pressure. The plane-wave approximation involves setting $p_s = \rho c v_s$ on the surface where p_s and v_s are the scattered pressure and normal velocity respectively. For a rigid body the scattered and incident normal velocities on the surface are related by $v_s = -v_{inc}$. Thus, the plane wave approximation reduces to setting $p_s = -\rho c v_{inc}$ on the surface. The far-field scattered pressure can be obtained from the approximate values of p_s and v_s on the surface. The normalized scattered pressure used in this report is very similar to the form function which is defined to be the magnitude of the ratio of the scattered pressure to the geometric acoustics approximation of the scattered pressure. In fact, for a sphere, the two normalizations are exactly the same. The normalized frequency ka is defined by $ka = 2\pi f a/c$ where f is the frequency, a is the mean radius, and c is the sound speed in water. The solid curve represents computed values at ka increments of 0.025 with no interpolation. The dotted curve (which is almost indistinguishable from the solid curve) corresponds to CHIEF computations at ka increments of 0.2 with interpolation to 0.025 increments.This curve represents CHIEF computations at only 10 ka values out of a total of 71. There is essentially no loss of accuracy in this frequency range for this degree of interpolation. It should be noted that the final frequency resolution is not limited to the value $ka = 0.025$ used in this example. Interpolation can be performed to any desired frequency resolution without any further CHIEF computations.

Figure 4 shows a similar comparison for CHIEF ka increments of 0.4 . This represents only six CHIEF frequency computations in this frequency range. Again the agreement is very good showing little loss of accuracy due to the frequency interpolation. Figure 5 shows another comparison corresponding to ka increments of 1.0 in CHIEF. Although the agreement is still not bad, the accuracy has deteriorated somewhat in the upper portion of the frequency band.

Figure 6 illustrates the importance of scaling the components of the CHIEF A and B matrices by $e^{-ikr_{mn}}$. The solid curve again represents calculations at ka increments of 0.025 with no interpolation. The dotted curve represents ka increments of 0.4 for the CHIEF computations with interpolation performed on the A and B matrices directly without any scaling. It is clear that the agreement is not nearly as good as it was for the scaled interpolation case shown in figure 4.

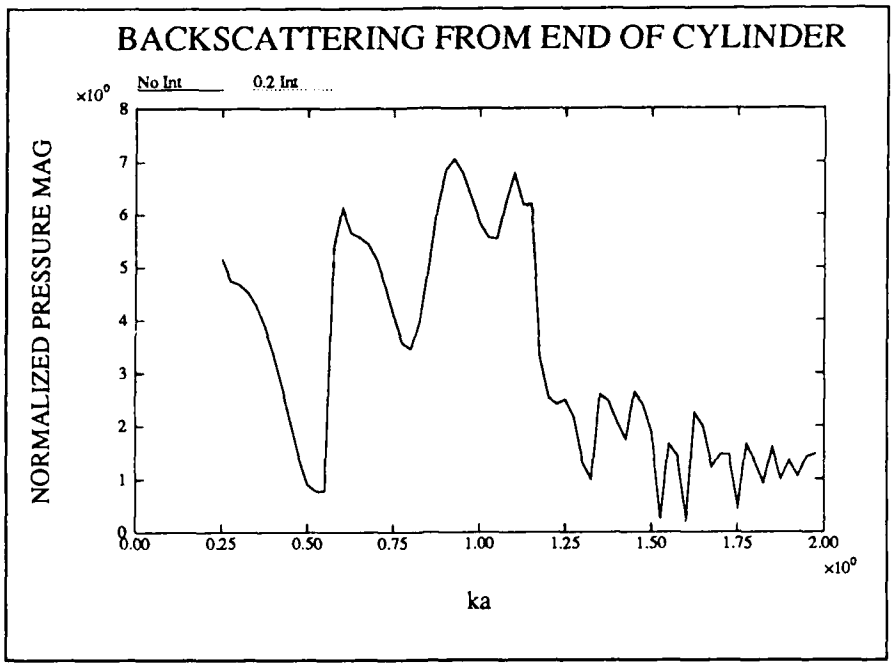

Figure 3. Backscattering from capped cylinder, CHIEF ka increment of 0.2.

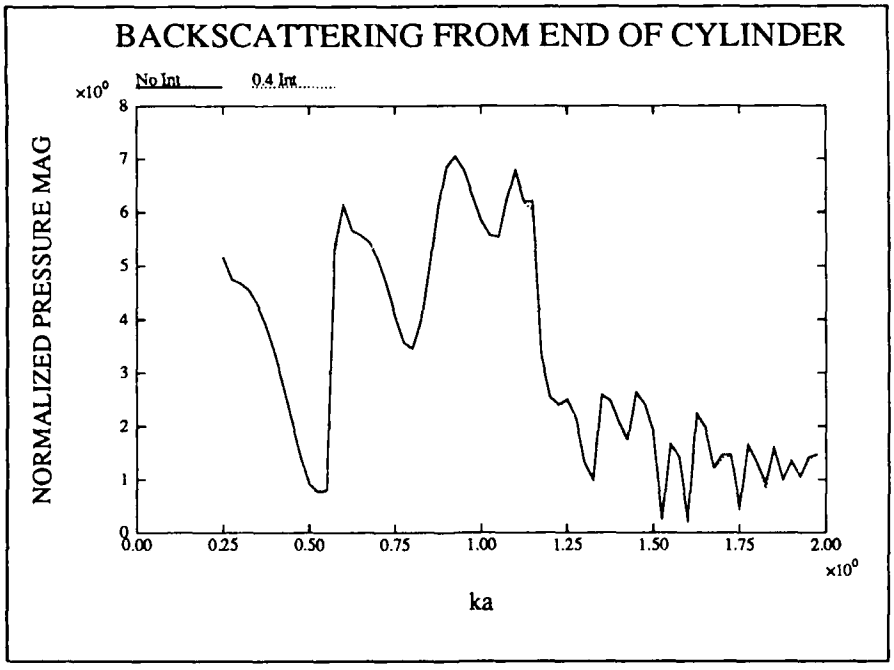

Figure 4. Backscattering from capped cylinder, CHIEF ka increment of 0.4.

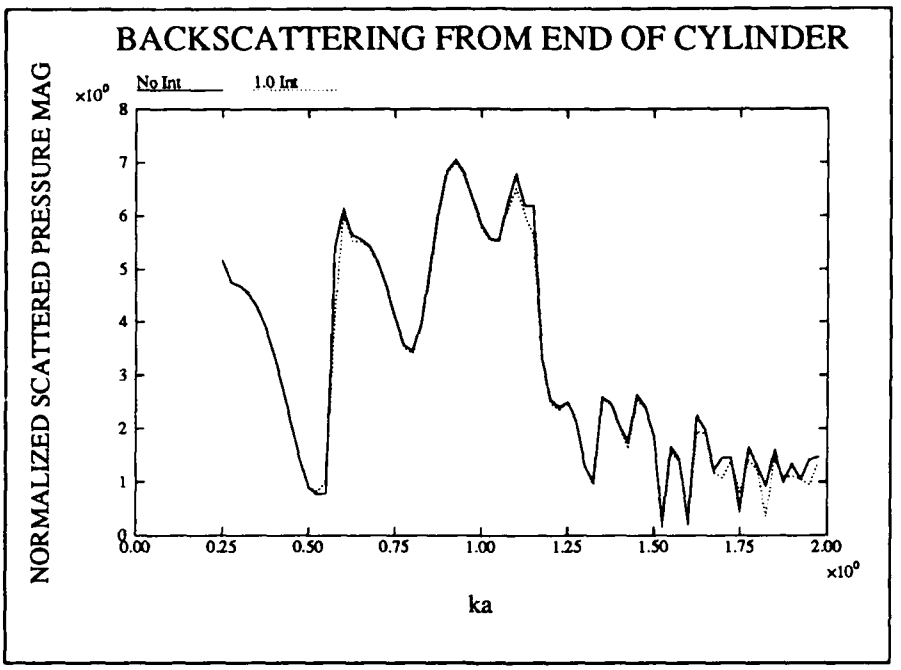

Figure 5. Backscattering from capped cylinder, CHIEF ka increment of 1.0.

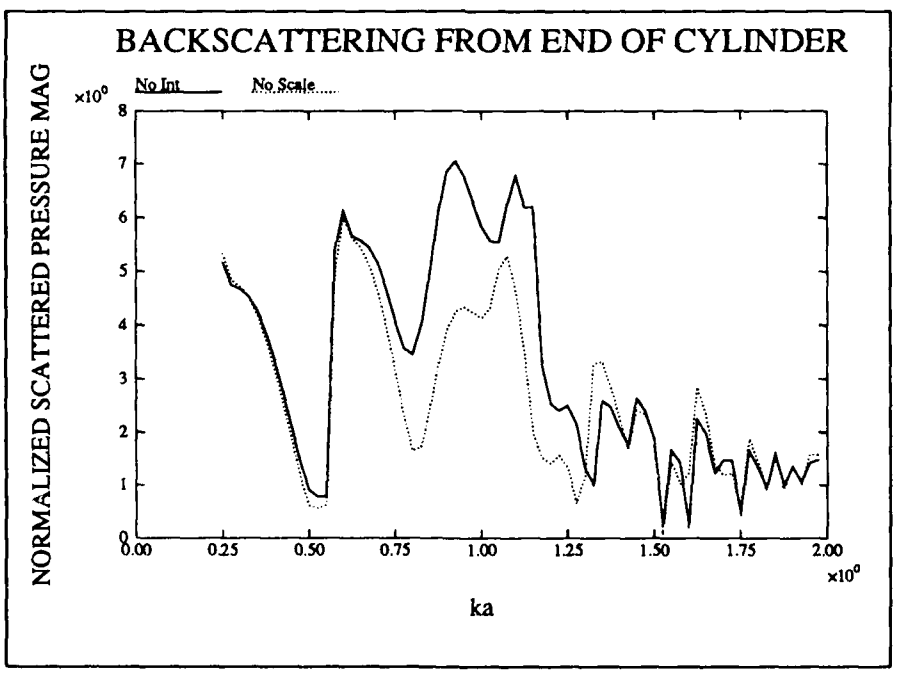

Figure 6. Effect of scaling on frequency interpolation.

CONCLUSIONS AND RECOMMENDATIONS

For coupled structural acoustic scattering problems, the spectral response often varies rapidly over a large dynamic range, requiring the response to be calculated at many closely spaced frequencies. In such problems, the computation time is often dominated by the calculation of acoustic interactions which do not vary rapidly with frequency. It has been shown in this report that large savings in computation time can be achieved without significant loss of accuracy by interpolating on appropriately scaled intermediate acoustic quantities. These quantities are computed on a coarse frequency grid and then interpolated to any desired frequency resolution in order to obtain the final response. The overall savings in computation time is typically more than an order of magnitude.

It is recommended that this frequency interpolation technique be incorporated in other similar computer codes dealing with structural acoustic scattering problems.

REFERENCES

Benthien, G., D. Barach, and D. Gillette. 1988. *CHIEF Users Manual*, NOSC Technical Document 970, revision 1.

Schenck, H.A. 1968. "Improved Integral Formulation for Acoustic Radiation Problems." *J. Acoust. Soc. Am.* 44:41–58.

Schenck, H.A., and G.W. Benthien. 1989. *Numerical Solution of Acoustic-Structure Interaction Problems*, NOSC Technical Report 1263.

Zienkiewicz, O.C. 1977. *The Finite Element Method*, Third Edition, McGraw-Hill, chapter 3.

INITIAL DISTRIBUTION

Naval Research Laboratory
Washington, DC 20375-5000
Dr. J. Bucaro
Dr. L. Dragonette
L. Shuetz

Naval Research Laboratory
Underwater Sound Reference Detachment
Orlando, FL 32856
Code 5970 (R. Timme)
Code 5976 (C. Siders)
Code 5976 (R. Montgomery)

David Taylor Research Center
Bethesda, MD 20084-5000
Dr. Y.N. Liu
M. Rummerman

Naval Underwater Systems Center
New London Laboratory
New London, CT 06320-5594
Code 2131 (J. Blottman)
Code 2132 (K. Webman)
Code 3234 (J. Lindberg)
Code 3322 (D. Bostian)
R. Radlinski
A. Carlson

Naval Sea Systems Command
Washington, DC 20362-5105
Code 55N2 (Dr. P.N. Majumdar)

Naval Surface Warfare Center Detachment
White Oak Laboratory
Silver Springs, MD 20903-5000
Dr. G. Gaunnard

Office of Naval Research
Arlington, VA 22217-5000
Code 1111 (John Lavery)

Naval Postgraduate School
Monterey, CA 93943
Prof. O.B. Wilson
Prof. Steve Baker

Catholic University of America
Washington, DC 20017
Prof. H. Uberall

University of Delaware
Newark, DE 19716
Prof. Robert P. Gilbert
Prof. George C. Hsiao
Prof. Ralph E. Kleinman

University of Colorado
Boulder, CO 80309-0449
Prof. Subhendu K. Datta

Georgia Institute of Technology
Atlanta, GA 30332
Prof. Jerry H. Ginsberg

Eastern Michigan University
Ypsilanti, MI 48197
James C. Porter

University of Kentucky
College of Engineering
Lexington, KY 40506-0046
Prof. A.F. Seybert

University of Texas at Austin
Austin, TX 78713-8029
Deborah A. Summa
Dr. Clark Penrod

University of Washington
Seattle, WA 98105
H.G. McMichael
N. Walden Barcus

Wayne State University
Detroit, MI 48202
Prof. X.F. Wu

AT&T Bell Laboratories
Whippany Road
Whippany, NJ 07981
Frank M. Labianca
Dr. David S. Burnett

INITIAL DISTRIBUTION (Continued)

Bendix Corporation
Oceanics Division
15825 Roxford Street
Sylmar, CA 91342-3597
Scott A. Hudson

Boeing Commercial Aircraft Company
A Division of the Boeing Company
P.O. Box 3707
Seattle, WA 98124-2207
Dr. G. Sengupta

Bolt, Baranek & Newman, Inc.
4015 Hancock Street, Suite 101
San Diego, CA 92110
Dr. Joel Young

General Electric Company
P.O. Box 4840
Syracuse, NY 13221
Michael H. Trent FRPI-A6
Leonard Longo EP5-F2

Global Associates, LTD
Engineering & Management Services
Number 4 Station Square
1423 Powhatan Street
Alexandria, VA 22314
Michael E. Buckman

Gould, Inc.
Ocean Systems Division
18901 Euclid Avenue
Cleveland, OH 44117
Stephen E. Hess

Hazeltine Corporation
115 Bay State Drive
Braintree, MA 02184
R. Grimes-Graeme

Honeywell, Inc.
6500 Harbour Heights Parkway
Everett, WA 98204-8899
Dr. Manuel Gonzales
Murray Simon

Hydroacoustics, Inc.
999 Lehigh Station Road
P.O. Box 23447
Rochester, NY 14692
Dr. R.F. Delacroix
Dr. J.V. Bouyoucos

Image Acoustics, Inc.
P.O. Box 6
N. Marshfield, MA 02059
Dr. John L. Butler

Rockwell International
3370 Mira Loma Avenue
P.O. Box 4921
Anaheim, CA 92803-4921
Charles P. Frahm

Sanders Associates, Inc.
H.W. Pope Technical Park #1
65 River Road, CS 907
Hudson, NH 03051-0907
Peter Harvey

Schlumberger
Old Quarry Road
Ridgefield, CT 06887-4108
Sergio Kostek

Science Applications International Corp.
803 West Broad Street, Suite 300
Falls Church, VA 22046
Georgio Borgiotti

SRI International
333 Ravenswood Avenue
Menlo Park, CA 94025
D. Kent Peterson

Texas Research Institute
9063 Bee Caves Road
Austin, TX 78733
L. Smith

Westinghouse Electric Corporation
P.O. Box 1488, MS 9845
Annapolis, MD 21404
L. Rowe

REPORT DOCUMENTATION PAGE

Form Approved OMB No. 0704-0188

1. AGENCY USE ONLY *(Leave blank)*	2. REPORT DATE	3. REPORT TYPE AND DATES COVERED
	November 1989	Final

4. TITLE AND SUBTITLE

APPLICATION OF FREQUENCY INTERPOLATION TO ACOUSTIC-STRUCTURE INTERACTION PROBLEMS

5. FUNDING NUMBERS

PE: 0602314N
RJ14B53
WU: DN308107

6. AUTHOR(S)

G. W. Benthien

7. PERFORMING ORGANIZATION NAME(S) AND ADDRESS(ES)

Naval Ocean Systems Center
San Diego, CA 92152-5000

8. PERFORMING ORGANIZATION REPORT NUMBER

NOSC TR 1323

9. SPONSORING/MONITORING AGENCY NAME(S) AND ADDRESS(ES)

Naval Research Laboratory
Washington, D.C. 20375-5000

10. SPONSORING/MONITORING AGENCY REPORT NUMBER

11. SUPPLEMENTARY NOTES

12a. DISTRIBUTION/AVAILABILITY STATEMENT

Approved for public release; distribution is unlimited.

12b. DISTRIBUTION CODE

13. ABSTRACT *(Maximum 200 words)*

For coupled structural acoustic scattering problems, the spectral response often varies rapidly over a large dynamic range, requiring the response to be calculated at many closely spaced frequencies. In such problems, the computation time is often dominated by the calculation of acoutic interactions which do not vary rapidly with frequency. It is shown in this report that large savings in computation time can be achieved without significant loss of accuracy by interpolating on appropriately scaled intermediate acoustic quantities. These quantities are computed on a coarse frequency grid and then interpolated to any desired frequency resolution in order to obtain the final response. The overall savings in computation time is typically more than an order of magnitude.

14. SUBJECT TERMS

acoustics
acoustic scattering
vibration of structures
target strength

15. NUMBER OF PAGES

24

16. PRICE CODE

17. SECURITY CLASSIFICATION OF REPORT	18. SECURITY CLASSIFICATION OF THIS PAGE	19. SECURITY CLASSIFICATION OF ABSTRACT	20. LIMITATION OF ABSTRACT
UNCLASSIFIED	UNCLASSIFIED	UNCLASSIFIED	UNLIMITED